International Journal of Thermophysics, Vol. 28, No. 4, August 2007 (© 2007)
DOI: 10.1007/s10765-007-0207-x

Unsteady Natural Convection Fluid Flow in a Vertical Microchannel under the Effect of the Dual-Phase-Lag Heat-Conduction Model

A. F. Khadrawi[1,2] and M. A. Al-Nimr[3]

Received: October 23, 2006

The unsteady hydrodynamics and thermal behavior of fluid flow in an open-ended vertical parallel-plate microchannel are investigated semi-analytically under the effect of the dual-phase-lag heat conduction model. The model that combines both the continuum approach and the possibility of slip at the boundary is adopted in the study. The effects of the Knudsen number *Kn*, the thermal relaxation time τ_q, and the thermal retardation time τ_T on the microchannel hydrodynamics and thermal behavior are investigated using the dual-phase-lag and hyperbolic-heat-conduction models. It is found that as *Kn* increases the slip in the hydrodynamic and thermal boundary condition increases. Also, the slip in the hydrodynamic behavior increases as τ_T and τ_q decrease, but the effect of τ_T and τ_q on the slip of the thermal behavior is insignificant.

KEY WORDS: dual-phase-lag heat conduction; microchannel thermal and hydrodynamic behavior; microscopic heat conduction models in microchannel; natural convection; vertical microchannel.

1. INTRODUCTION

The fluid flow in microchannels has become an attractive area of research during the last few years. This is due to new applications of the microchannel flow in micro-pumps, micro-turbines, micro-heat exchangers,

[1] Department of Mechanical Engineering, Al-Balqa' Applied University, Al-Salt, Jordan.
[2] To whom correspondence should be addressed. E-mail: khadrawi99@yahoo.com
[3] Department of Mechanical Engineering, Jordan University of Science and Technology, P.O. Box 3030, Irbid 22110, Jordan.

and other micro-components. Extensive experimental and theoretical studies have been made in this area in order to understand the fluid behavior within these micro-devices [1–27].

It has been reported that phenomena in micro-geometry may differ from those in macroscopic counterparts. A dimensionless parameter that distinguishes between the fluid flow in macro-channels from that in microchannels is the Knudsen number [22–27]. This number represents the ratio of the mean free path length of the fluid to the characteristic length of the fluid domain. The Knudsen number ($Kn = \lambda/L$) is used to indicate the degree of flow rarefaction or the scale of the flow problem. Rarefaction or microscale effects are ignored by the Navier–Stokes equations, and these equations are therefore strictly accurate only at a vanishingly small $Kn (Kn < 0.001)$ [22–27]. The appropriate flow and heat transfer models depend on the range of the Knudsen number, and a classification of the different gas flow regimes is as follows: $Kn < 0.001$ for continuum flow, $0.001 < Kn < 0.1$ for slip flow, $0.1 < Kn < 10$ for transition flow, and $10 < Kn$ for free molecular flow [22–27].

In the slip flow regime, the continuum flow model is still valid for calculations of the flow properties away from solid boundaries. However, the boundary conditions have to be modified to account for the incomplete interaction between the gas molecules and the solid boundaries. In spite of the large amount of published research so far in the microchannel literature, many parts of the physical laws governing fluid flow and heat transfer in micro-geometries remain unknown [22–27]. Recently, discrepancies between microchannel flow behavior and macroscale Stokes flow theory have been summarized in a review [6]. It is widely accepted that the deviations observed in gas flows can be attributed to slip at the wall [7, 22–27], and several researchers have reported results for gas flows [8–12, 22–27].

In parallel to the breakdown of the continuum flow approach and the no-slip boundary condition from hydrodynamics and a thermal point of view, the classical diffusion energy equation, based on Fourier's law, does not apply well in micro-devices. The thermal behavior of microchannels has been extensively investigated by many researchers using different models, designs, and geometrical and operating parameters. Most of these studies are based on the parabolic (diffusion) heat-conduction model. The parabolic-heat-conduction model is able to describe the thermal behavior of these microchannels in many practical applications. However, there are numerous cases in which the utilization of the hyperbolic or the dual-phase-lag heat-conduction models becomes essential [13, 22]. Transient free convection fluid flow in a vertical microchannel was investigated by the present authors [23], but using the hyperbolic heat-conduction model. We refer the reader to Refs. 22 and 23, which summarize these applications

and illustrate the mathematical background of the dual-phase-lag heat-conduction model. The basics of this model are summarized here [22]. Cattaneo [14] and Vernotte [15] suggested independently a modified heat flux model in the form [22],

$$\vec{q}\left(t+\bar{\tau}_q,\vec{r}\right)=-k\vec{\nabla}T\left(t,\vec{r}\right) \tag{1}$$

where $\vec{q}$ is the heat flux vector, k is the thermal conductivity, and $\bar{\tau}_q$ is the phase-lag in the heat flux vector. The constitutive law of Eq. (1) assumes that the heat flux vector (the effect) and the temperature gradient (the cause) across a material volume occur at different instants of time, and the time delay between the heat flux and the temperature gradient is the relaxation time $\bar{\tau}_q$. To remove the preceding assumption made in the thermal wave model, as proposed in Eq. (1), the dual-phase-lag model is proposed [16–18]. The dual-phase-lag model allows either the temperature gradient (cause) to precede the heat flux vector (effect) or the heat flux vector (cause) to precede the temperature gradient (effect) in the transient process. Mathematically, this can be represented by [19–22]

$$\vec{q}\left(t+\bar{\tau}_q,\vec{r}\right)=-k\vec{\nabla}T\left(t+\bar{\tau}_T,\vec{r}\right) \tag{2}$$

where $\bar{\tau}_T$ is the phase-lag in the temperature gradient vector and $\bar{\tau}_q$ is the phase-lag in the heat flux vector. For the case of $\bar{\tau}_T > \bar{\tau}_q$, the temperature gradient established across a material volume is a result of the heat flow, implying that the heat flux vector is the cause and the temperature gradient is the effect. For $\bar{\tau}_T < \bar{\tau}_q$, on the other hand, heat flow is induced by the temperature gradient established at an earlier time, implying that the temperature gradient is the cause, while the heat flux vector is the effect. In the absence of the temperature gradient phase-lag ($\bar{\tau}_T = 0$), Eq. (2) reduces to the classical hyperbolic heat-conduction equation as described by Eq. (1). Also, in the absence of the two phase-lags ($\bar{\tau}_T = \bar{\tau}_q = 0$), Eq. (2) reduces to the classical diffusion equation employing Fourier's law. Due to this lagging response, both the hyperbolic and dual-phase-lag heat-conduction models have been receiving increasing attention as compared to the classical diffusion model, which assumes an immediate response between the heat flux vector and the temperature gradient.

Khadrawi and Al-Nimr [22,23] investigated the thermal behavior of a stagnant gas confined in a horizontal microchannel as described by the dual-phase-lag heat-conduction model and transient free convection fluid flow in a vertical microchannel as described by the hyperbolic heat-conduction model.

The objective of this study is to investigate the microchannel transient thermal behavior under the effect of the dual-phase-lag heat-conduc-

tion model. The model that combines the continuum approach with slip at the boundaries is adopted in this investigation. The effects of the Knudsen number, the phase-lag in the heat flux, and the phase-lag in temperature gradients on the deviations among the three heat conduction models are investigated.

2. ANALYSIS

Consider an unsteady, laminar, fully developed, free convection flow inside an open-ended, vertical, parallel-plate microchannel. The fluid is assumed to be Newtonian with uniform properties. Also, it is assumed that both viscous dissipation and internal heat generation are absent. Referring to Fig. 1 and using the dimensionless parameters given in the nomenclature, the governing equations of the hydrodynamic and thermal behavior, as described by the dual-phase-lag heat-conduction model, are given as [16–22]

$$\frac{\partial U}{\partial \eta} = \theta + \frac{\partial^2 U}{\partial Y^2} \tag{3}$$

$$\frac{\partial \theta}{\partial \eta} = -\frac{1}{Pr}\frac{\partial Q}{\partial Y} \tag{4}$$

$$Q + \tau_q \frac{\partial Q}{\partial \eta} = -\left(\frac{\partial \theta}{\partial \xi} + \tau_T \frac{\partial^2 \theta}{\partial \eta \partial \xi}\right) \tag{5}$$

Equations (3)–(5) assume the following initial and boundary thermal conditions [22,23]

$$\theta(0, Y) = U(0, Y) = 0 \tag{6a}$$

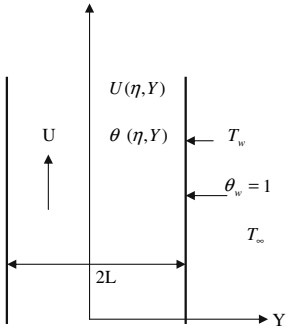

Fig. 1. Schematic diagram of the problem under consideration.

$$U(\eta, 1) = -\Omega Kn \frac{\partial U}{\partial Y}(\eta, 1) \tag{6b}$$

$$\frac{\partial U}{\partial Y}(\eta, 0) = 0 \tag{6c}$$

$$\frac{\partial \theta}{\partial Y}(\eta, 0) = 0 \tag{6d}$$

$$\theta(\eta, 1) - 1 = Kn \frac{\psi}{Pr} Q(\eta, 1) \tag{6e}$$

where $\Omega = \frac{2-\sigma_v}{\sigma_v}$, $\psi = \frac{2-\sigma_T}{\sigma_T}\left(\frac{2\gamma}{\gamma+1}\right)$, and $Kn = \frac{\lambda}{L}$ (Knudsen number)

Also, the dimensionless slip-flow and temperature-jump boundary conditions are given as, respectively,

$$\Delta U|_{\text{wall}} = U(\eta, 1) = -\Omega Kn \frac{\partial U}{\partial Y}(\eta, 1)$$

and

$$\Delta\theta|_{\text{wall}} = \theta(\eta, 1) - 1 = Kn \frac{\psi}{Pr} Q(\eta, 1),$$

where the right-hand side of Eqs. (6b) and (6e) represents the slip in the hydrodynamic and thermal boundary conditions of the boundary.

It is worth mentioning that Eqs. (3)–(5) are reduced to the hyperbolic heat conduction model when $\tau_T = 0$. The appearance of τ_T in Eq. (3) allows the heat flux to be the cause or the effect depending on the values of τ_T and τ_q. For the case of $\tau_T > \tau_q$, the temperature gradient established across a material volume is a result of the heat flow, implying that the heat flux vector is the cause and the temperature gradient is the effect. For $\tau_T < \tau_q$, on the other hand, heat flow is induced by the temperature gradient established at an earlier time, implying that the temperature gradient is the cause, while the heat flux vector is the effect. Tzou 13 provided experimental values for τ_T where $\tau_T \sim 100\tau_q$ for most known metals.

However, the effect of τ_T and τ_q on the microchannel thermal behavior may be significant within the very early stage of time, i.e., when $\eta \ll \tau_T$ and $\eta \ll \tau_q$. This may be shown by rewriting Eq. (5) in the following form:

$$Q + \frac{\partial Q}{\partial\left(\frac{\eta}{\tau_q}\right)} = -\left(\frac{\partial \theta}{\partial \xi} + \frac{\partial^2 \theta}{\partial\left(\frac{\eta}{\tau_T}\right)\partial \xi}\right) \tag{6f}$$

In order for the second and fourth terms in Eq. (6f) to have significant effect, the denominators must be very small, i.e., $\frac{\eta}{\tau_q} \ll 1$ and $\frac{\eta}{\tau_T} \ll 1$

Equations (3)–(6) are solved using the Laplace transformation technique. Now with the notation that $L\{\theta(\eta, Y)\} = W(S, Y)$, $L\{Q(\eta, Y)\} = V(S, Y)$, and $L\{U(\eta, Y)\} = F(S, Y)$, the Laplace transformation of Eqs. (3)–(6) yields

$$SF = W + \frac{d^2F}{dY^2} \tag{7}$$

$$SW = -\frac{1}{Pr}\frac{dV}{dY} \tag{8}$$

$$V + \tau_q SV = -\frac{dW}{d\xi} - \tau_T S\frac{dW}{d\xi} \tag{9}$$

Also, the Laplace transformation of the boundary conditions is given as

$$\begin{aligned} \frac{\partial F}{\partial Y}(S, 0) &= 0 \\ F(S, 1) &= -\Omega Kn\frac{\partial F}{\partial Y}(S, 1) \\ \frac{\partial W}{\partial Y}(S, 0) &= 0 \\ W(S, 1) - \frac{1}{s} &= Kn\frac{\psi}{Pr}V(S, 1) \end{aligned} \tag{10}$$

According to the boundary conditions given in Eq. (10), Eqs. (7)–(9) are solved to give

$$W = \frac{-C}{SPr}\beta\cosh(\beta Y) \tag{11}$$

$$V = C\sinh(\beta Y) \tag{12}$$

$$F = C_1\cosh(\sqrt{S}Y) + C_2\cosh(\beta Y) \tag{13}$$

where $C = \frac{-1/S}{\left[\frac{\beta}{SPr}\cosh(\beta) + Kn\frac{\psi}{Pr}\sinh(\beta)\right]}$, $C_2 = \frac{C\beta}{[(\beta^2 - S)SPr]}$, $C_1 = \frac{-C_2[\cosh(\beta) + \Omega Kn\beta\sinh(\beta)]}{\left[\cosh\left(\sqrt{S}\right) + \Omega Kn\sqrt{S}\sinh\left(\sqrt{S}\right)\right]}$ and $\beta = \sqrt{\frac{SPr(1+\tau_q S)}{(1+\tau_T S)}}$

Equations (11)–(13) are inverted in terms of the Riemann-sum approximation [13] as

$$\theta(\eta, Y) \cong \frac{e^{\varepsilon\eta}}{\eta}\left[\frac{1}{2}W(\varepsilon, Y) + \mathrm{Re}\sum_{n=1}^{N} W\left(\varepsilon + \frac{in\pi}{\eta}, Y\right)(-1)^n\right] \tag{14}$$

where Re refers to the "real part of" and $i = \sqrt{-1}$ is the imaginary number, N is the number of terms used in the Riemann-sum approximation, and ε is the real part of the Bromwich contour that is used in inverting Laplace transforms. The Riemann-sum approximation for the Laplace

inversion involves a single summation for the numerical process. Its accuracy depends on the value of ε and the truncation error dictated by N. The value of ε must be selected so that the Bromwich contour encloses all the branch points [1]. For faster convergence, however, numerous numerical experiments have shown that a value satisfying the relation $\varepsilon\eta \cong 4.7$ gives the most satisfactory results [15]. Hence, the appropriate value of ε for faster convergence depends on the instant of time (η) at which the lagging phenomenon is studied. The criterion shown by $\varepsilon\eta \cong 4.7$ is independent of the value of η. The number N of terms used in the Riemann-sum is determined. Thus, a prescribed threshold for the accumulated partial sum is satisfied at given values of ε, Y, and η.

3. RESULTS AND DISCUSSION

Figure 2 shows the effect of the Knudsen number *Kn* on the spatial temperature distribution. As shown from this figure, an increase in *Kn* yields an increase in the temperature jump at the heated wall. This is due to the reduction in the interaction between the gas molecules and the heated wall. As *Kn* increases, the mean free path length of the gas molecules increases which implies that any molecule reflected from the wall has less opportunity to collide with other molecules and

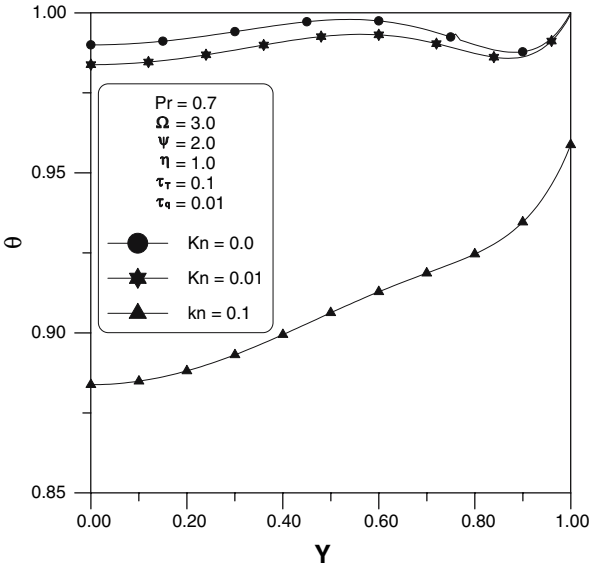

Fig. 2. Spatial temperature distribution for different *Kn*.

then to transmit it to the wall heating effect. A larger *Kn* implies fewer molecules collide with the wall and carry part of its heating effect. Because of increasing the temperature jump at the wall, less heat is transmitted to the gas, which yields less buoyancy driving force. This produces low-temperature profiles at higher *Kn* as shown in Fig. 2.

The effects of τ_q and τ_T on the temperature spatial distribution is shown in Figs. 3 and 4, respectively. An increase in the thermal relaxation time τ_q and the thermal retardation time τ_T yields an increase in the gas temperature, especially at a location far from the heated wall. An increase in τ_q implies that the temperature response (the effect) precedes the heat flux (the cause), and an increase in τ_T implies that the heat flux (the cause) precedes the temperature response (the effect). As a result, any increase in τ_q yields an increase in the temperature distribution at the same time.

Figure 5 shows the effect of *Kn* on the velocity spatial distribution. As *Kn* increases, the velocity slip at the wall increases, which reduces the retarding effect of the wall. This yields an observable increase in the gas velocity near the wall. However, as *Kn* increases, the temperature jump increases and this reduces the amount of heat transfer from the wall to the fluid. This reduction in heat transfer reduces the buoyancy effect, which drives the flow and hence reduces the gas velocity far from the wall. The reduction in veloc-

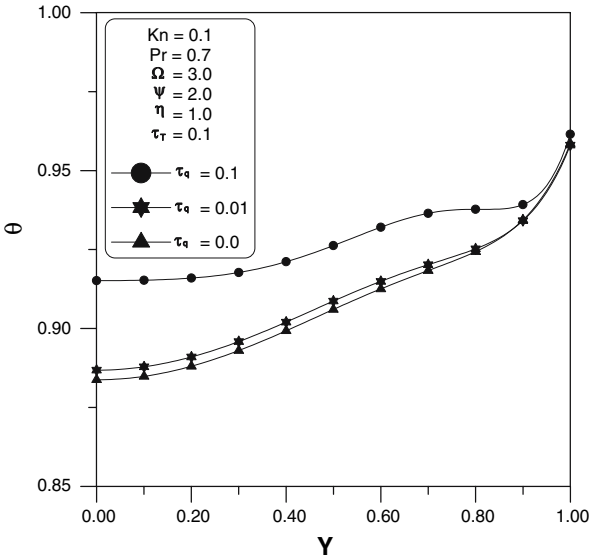

Fig. 3. Spatial temperature distribution at different τ_q.

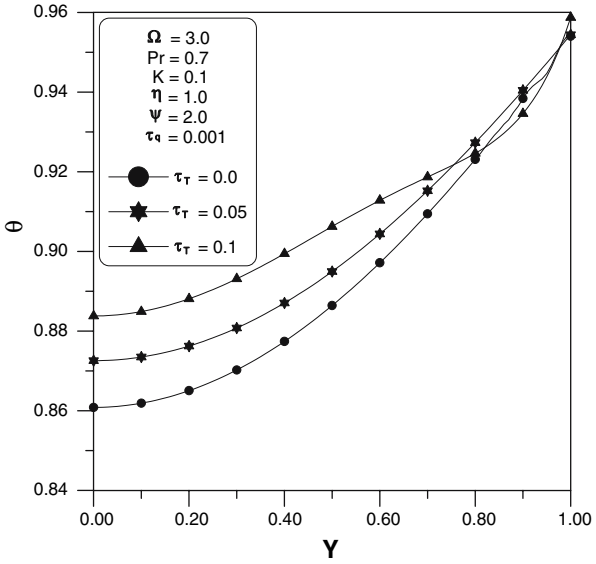

Fig. 4. Spatial temperature distribution at different τ_T.

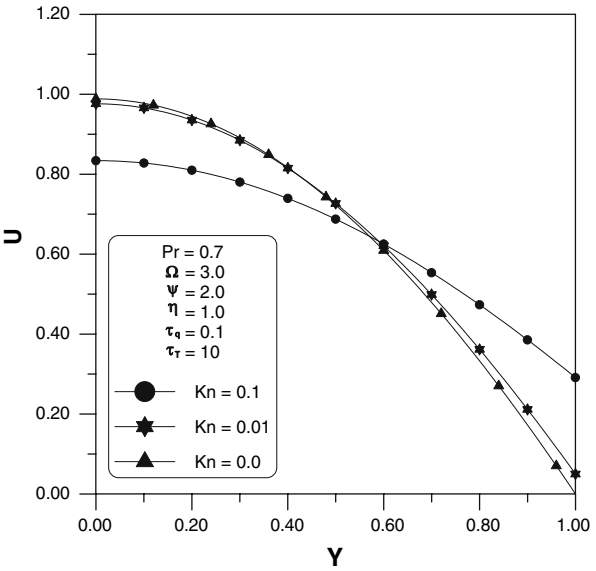

Fig. 5. Spatial velocity distribution for different *Kn*.

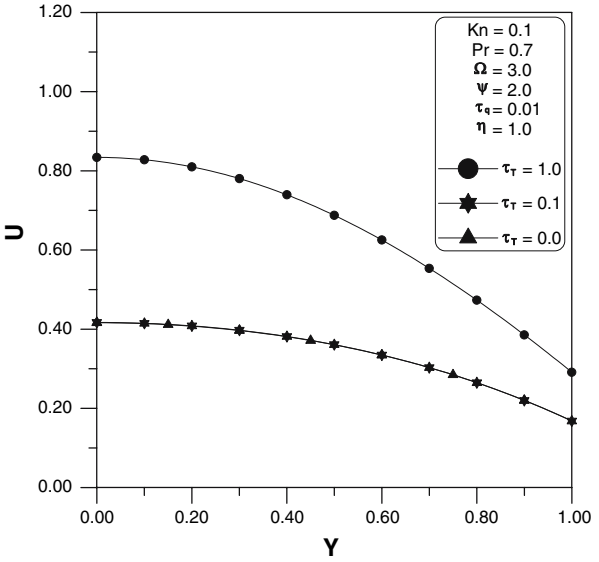

Fig. 6. Spatial velocity distribution at different τ_T.

ity due to the reduction in heat transfer is offset by the increase in U due to the reduction in the frictional retarding forces near the wall.

The effect of the thermal retardation time τ_T on the velocity spatial distribution is shown in Fig. 6. It is clear that as τ_T increases, the slip in the hydrodynamics boundary condition increases.

The effect of Kn on the transient behavior of the wall temperature jump is shown in Fig. 7. It is clear that the temperature jump increases as Kn increases, as explained previously. Also, it is clear that the temperature jump decreases as time proceeds and then approaches very small, but nonzero, asymptote especially at large values of Kn. As time proceeds, the heating effect of the wall raises the gas temperature and the difference between the wall and the adjacent gas temperatures decreases.

The effect of τ_T on the velocity difference at the wall is shown in Fig. 8. It is clear that as τ_T decreases the velocity jump at the wall increases, especially at large values of Kn.

The effect of τ_T on the transient behavior of the velocity slip at the wall is shown in Fig. 9. As predicted, the velocity slip increases as τ_T decreases and as time proceeds. As time proceeds, the gas temperature increases and raises the gas velocity due to the buoyancy effect. As a result, the difference between the adjacent gas velocity and the wall zero

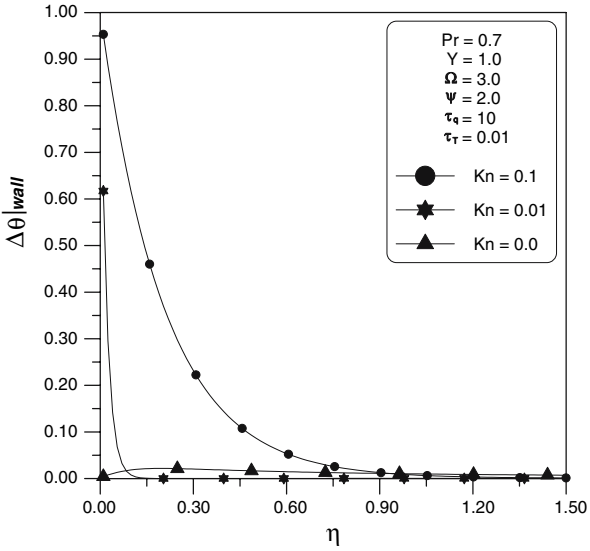

Fig. 7. Effect of *Kn* on the transient temperature difference at the wall.

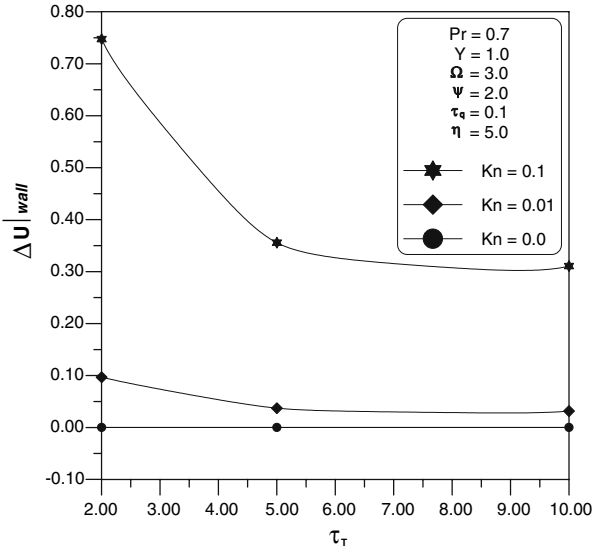

Fig. 8. Effect of τ_T on the velocity difference at the wall.

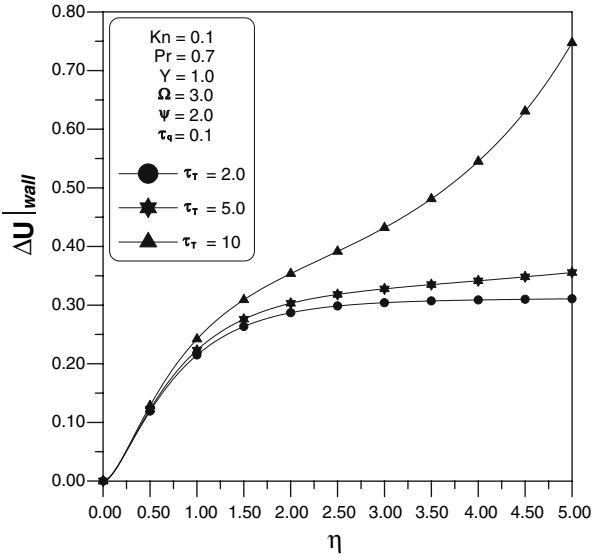

Fig. 9. Effect of τ_T on the transient velocity difference at the wall.

velocity increases. Also, it is clear that flow needs more time to reach steady-state behavior as τ_T increases.

4. CONCLUSIONS

The transient hydrodynamics and thermal behavior of fluid flow in an open-ended, vertical, parallel-plate microchannel are investigated analytically under the effect of the dual-phase-lag heat-conduction model. The microchannel hydrodynamics and thermal behavior are affected by three parameters Kn, τ_q, and τ_T. It is found that as Kn increases the slip in the hydrodynamic and thermal boundary condition increases. Also, the slip in the hydrodynamic behavior increases as τ_T and τ_q decrease, but the effect of τ_T and τ_q on the thermal behavior is insignificant.

Nomenclature

c	specific heat, $\mathrm{J \cdot kg^{-1} \cdot K^{-1}}$
F	Laplace transformation of the dimensionless velocity
Kn	Knudsen number, λ/L
k	thermal conductivity, $\mathrm{W \cdot m^{-1} \cdot K^{-1}}$
L	characteristic length, m
Pr	Prandtl number, ν/α

q conduction heat flux, $\mathrm{W \cdot m^{-2}}$
q_{o} reference conduction heat flux, $k\Delta T/L$
Q dimensionless conduction heat flux, q/q_o
S Laplacian domain
t time, s
T temperature, K
T_∞ ambient and initial temperature, K
T_{w} wall temperature, K
V Laplace transformation of the dimensionless heat flux
u axial velocity, $\mathrm{m \cdot s^{-1}}$
u_o reference velocity, $L^2 g\beta\,(T_{\mathrm{w}} - T_\infty)/\nu$
U dimensionless velocity, u/u_o
W Laplace transformation of the dimensionless temperature
y transverse coordinate, m

Greek symbols

α thermal diffusivity, $\mathrm{m^2 \cdot s^{-1}}$
ΔT dimensionless temperature difference, $T_{\mathrm{w}} - T_\infty$
ψ $= \frac{2-\sigma_T}{\sigma_T}\left(\frac{2\gamma}{\gamma+1}\right)$
η dimensionless time, $\nu t/L^2$
γ specific heat ratio
λ mean free path, m
ν kinematic viscosity, $\mathrm{m^2 \cdot s^{-1}}$
Ω $= \frac{2-\sigma_v}{\sigma_v}$
ρ density, $\mathrm{kg \cdot m^{-3}}$
σ_T thermal accommodation coefficient
σ_v tangential-momentum accommodation coefficient
θ dimensionless temperature, $(T - T_\infty)/(T_{\mathrm{w}} - T_\infty)$
$\bar{\tau}_T$ phase-lag in temperature gradient, s
$\bar{\tau}_q$ phase-lag in heat flux vector, s
τ_T dimensionless phase-lag in temperature gradient, $\bar{\tau}_T \alpha/L^2$
τ_q dimensionless phase-lag in heat flux vector, $\bar{\tau}_q \alpha/L^2$
Y dimensionless transverse coordinates, y/L

Subscripts

∞ ambient
w wall

REFERENCES

1. G. Karniadakis and A. Beskok, *Micro Flows: Fundamentals and Simulation*, (Springer-Verlag, New York, 2002).

2. Y. Zohar, *Heat Convection in Micro Ducts* (Kluwer, Boston, 2003).
3. Y. Zohar, W. Lee, S. Lee, L. Jiang, and P. Tong, *J. Fluid Mech.* **472**:125 (2002).
4. G. P. Duncan and G. P. Peterson, *Appl. Mech. Rev.* **47**:397 (1994).
5. N. T. Obot, *Microscale Thermophys. Eng.* **6**:155 (2002).
6. C. Ho and Y. Tai, *Ann. Rev. Fluid Mech.* **30**:579 (1998).
7. J. C. Shih, C. Ho, J. Liu, and Y. Tai, *Microelectromech. Syst. (MEMS)* **59**:197 (1996).
8. P. Wu and W. A. Little, *Cryogenics* **23**:273 (1983).
9. S. B. Choi, R. F. Barron, and O. R. Warrington, *Micromech. Sensors, Actuators, Syst.* **32**:123 (1991).
10. J. C. Harley, Y. Huang, H. Bau, and J. N. Zemel, *J. Fluid Mech.* **284**:257 (1995).
11. S. F. Choquette, M. Faghri, E. J. Kenyon, and B. Sunden, *Proc. Natl. Heat Transfer Conf.* **5**:25 (1996).
12. Z. Y. Guo and X. B. Wu, *Int. J. Heat Transfer* **40**:3251 (1997).
13. D. Y. Tzou, *Macro- to Microscale Heat Transfer: The Lagging Behavior* (Taylor and Francis, Washington, DC, 1997), pp. 1–64.
14. C. Cattaneo, *Compte Rendus* **247**:431 (1958).
15. O. Vernotte, *Compte Rendus* **252**:2190 (1961).
16. D. Y. Tzou, *ASME J. Heat Transfer* **117**:8 (1995).
17. Y. Tzou, *Int. J. Heat Mass Transfer* **38**:3231 (1995).
18. D. Y. Tzou, *AIAA J. Thermophys. Heat Transfer* **9**:686 (1995).
19. M. A. Al-Nimr and M. Naji, *Int. J. Thermophys.* **21**:281 (2000).
20. M. A. Al-Nimr and M. Naji, *Microscale Thermophys. Eng.* **4**:231 (2000).
21. M. A. Al-Nimr, M. Naji, and V. Arpaci, *ASME J. Heat Transfer* **122**:217 (2000).
22. M. A. Al-Nimr and A. F. Khadrawi, *Int. J. Thermophys.* **25**:1953 (2004).
23. A. F. Khadrawi, A. Othman, and M. Al-Nimr, *Int. J. Thermophys.* **26**:905 (2005).
24. O. Haddad, M. Abuzaid, and M. Al-Nimr, *Entropy* **6**:413 (2005).
25. O. Haddad, M. Al-Nimr, and M. Abuzaid, *Acta Mech.* (in press).
26. O. Haddad, M. Abuzaid, and M. Al-Nimr, *Numer. Heat Transfer* (in press)
27. O. Haddad, M. Al-Nimr, and Y. Taamneh, *J. Porous Media* (in press).